2nd International Symposium on Magnetic Beaing
July 12-14, 1990, Tokyo, Japan

COST-EFFECTIVE IMPLEMENTATION OF ACTIVE MAGNETIC BEARINGS

D. ZLATNIK and A. TRAXLER

Institute for Robotics, ETH Zürich, CH-8092 Zurich, Switzerland.

Abstract

A low-cost implementation of an active magnetic bearing (AMB) is achieved, using cheap Hall-effect sensors instead of displacement sensors, centralized digital control and signal processing on a single microcomputer, a modular structure using commercial components and in some cases, eliminating the need for a thrust bearing. Together with cost effectiveness the performance and overall reliability due to simplicity, are kept. An AMB for a crystal growth process was successfully integrated with the constraint of a wide gap between rotor and stator.

1. Introduction

The active magnetic bearing (AMB) as an inherently unstable plant requires feedback control. Possible approaches are feeding back the measured rotor displacement, flux, current or voltage, to produce controlled electromagnetic forces, acting on the rotor [5].

In most of the existing implementations of AMB's, a separate displacement measurement system ist used, which is expensive relatively to the overall system cost, because of high-quality "clean" measurement which is not always necessary and may even reject useful information [1].

In certain applications as in crystal-growth described later, system and environmental constrains force the mechanical design to allow a free axial movement of the rotor for handling, i.e. no axial bearing, and a wide gap between rotor and stator. An earlier work [2] describes an electro-permanent magnetic bearing for a similar application. In that approach, permanent magnets supply a passive axial stiffness, so an extra active axial bearing is also eliminated. The limitation of this approach is that the rotor axial degree of freedom is not controlled and not actively damped.

In this work we describe an AMB system for controlling the rotor's five degrees of freedom, using only radial AMB's and very cheap Hall-effect sensors for rotor position control. Following a brief description of the system concept, the mechanical construction, the displacement measurement and the control are described with simplified formulations. Finally an implementation of the AMB for a crystal growth process is presented.

2. System concept

An industrial or commercial product should be designed to be *functional, reliable, low-cost* and *adaptable within its environment.*

Reliability is based on simplicity and in AMB it is mainly achieved by use of reliable power-amplifiers and converting measurement signal processing and control realized in complex analog electronics, into software algorithms. A microcomputer, centralizing control and system operation, enables an on-line monitoring and diagnostics to predict or detect failure and apply emergency procedures.

Adaptation within the environment regards mainly to functionality inside a large-scale plant of identical units and noise problematics due to high current switching (fig. 1). A large-scale plant requires compatibility with the communication network for operational commands and monitoring done by the plant supervisor. Noise is reduced, using shielding and grounding to be effective in protecting both the system and the environment.

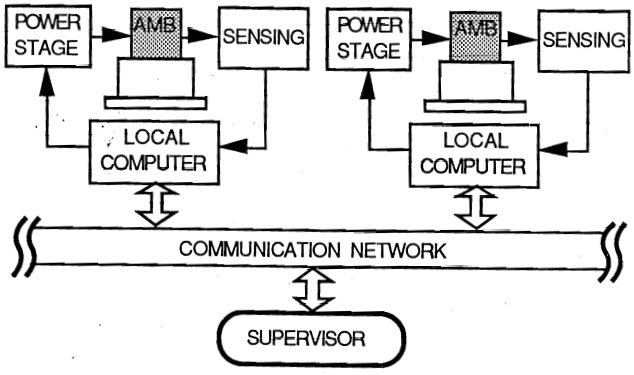

Fig. 1: *Large scale system*

The system operates in discrete "stable" states like STOP, FLOAT, ROTATE, CALIBRATE, DIAGNOSE. For example, ROTATE can be performed only if FLOAT is succesfull. Each of the states can be reached via the supervisor, through the communication network upon request or through an emergency procedure.

3. Mechanical setup of the AMB system.

The mechanical layout uf the AMB system includes two radial AMBs, **A** and **B** as described in fig. 2. Each bearing includes four electro-magnets. The rotor is held vertically by these bearings which apply both, radial and axial force components. The two bearings control five degrees of freedom of the rotor The rotation about the **Z** axis is controlled by a motor drive..

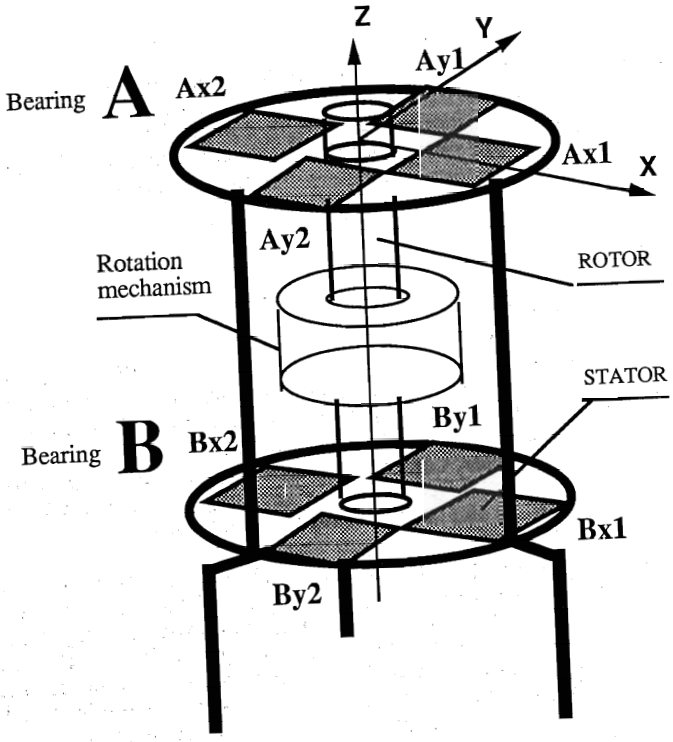

Fig. 2: *Mechanical setup of AMB System*

The cross-section of one electromagnet-pair is shown in fig. 3. The magnets are driven by the currents i_1 and i_2 and produce a magnetic flux in the U-shaped core. The flux-path is closed by an iron core attached to the rotor. The force, generated by the magnets can be separated into a radial and an axial component.

The currents through the coils of the magnets are generated by power amplifiers. The current in each coil is combined of two components, i_v, premagnetization current, also generating the axial force component, and i_x, the control current to control the radial force.

Based on the configuration of fig. 3, the total airgap g(x,z) can be expressed as

$$g(x,z) \cong x_0 \pm x + \sqrt{(x_0 \pm x)^2 + (z_0 \pm z)^2} \qquad (3.1)$$

where the sign of x regards to the left and right electromagnets, and the sign of z is general.

With the driving currents

$$i_1 = A_i\,(U_v + U_x) = i_v + i_x \qquad (3.2)$$

and

$$i_2 = A_i\,(U_v - U_x) = i_v - i_x \qquad (3.3)$$

the linearization in the working point $(i_x,i_v,x,z) = (0,i_{vo},0,0)$ leads to the force components

$$F_x \cong 2\,(K_i i_x + K_x x) + K_z z \qquad (3.4)$$

$$F_z \cong 2\,(F_0 + K_i i_v - K_z z) \qquad (3.5)$$

where F_x can be controlled with the control current i_x and the axial force F_z has to be controlled with the premagnetization current i_v which is therefore not constant as usual in AMB's. The constants K_i, K_x and K_z depends on i_{vo}.

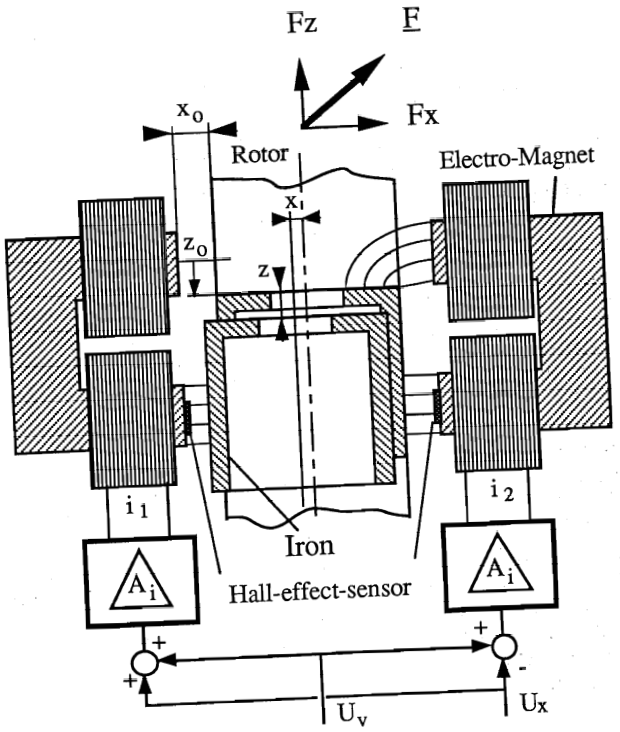

Fig. 3: *AMB pair cross-section and current drive*

In general, a complete layout includes two AMB's, controlling five degrees of freedom of the rotor. Depending on the application, the rotor can be mounted vertically or horizontally as shown in fig. 4. In the horizontal setup, the rotor cores are mounted to produce opposite controlled axial forces and in the vertical setup, they produce summed controlled axial forces, carrying the rotor weight.

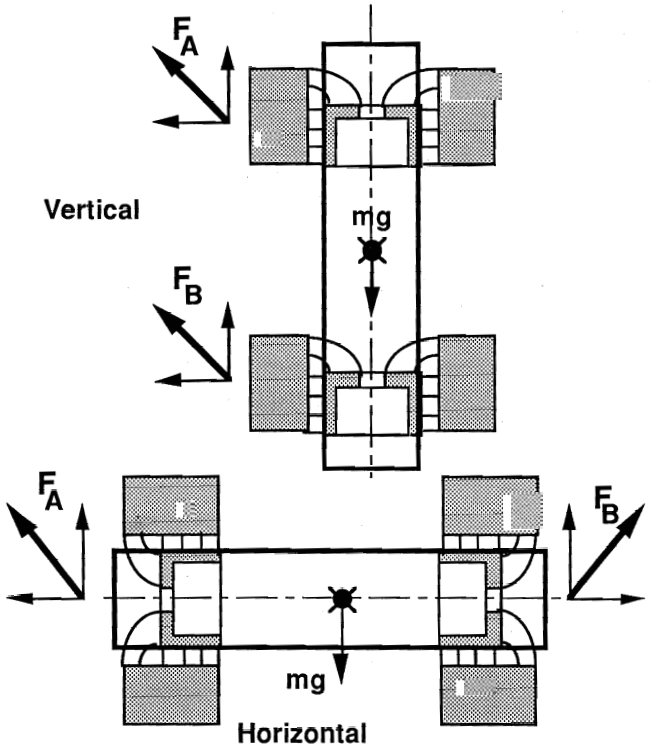

Fig. 4: *Vertical and horizontal constructions.*

4. Displacement measurement using Hall-effect sensors

The measurement of rotor displacement in an AMB is used in the closed-loop control to stabilize the rotor and to achieve the required stiffness. The displacement can be measured directly by using any kind of commercial gauge based on inductance, capacitance or optics. These gauges achieve good performance for small ranges and gaps. They occupy relatively large space and require dedicated electronics which increase the cost.

We here describe an alternative possibility, using Hall-effect sensors. They actually measure the flux density, which depends on the rotor displacement and the ampere-turns in the magnet coils. They show sufficient sensitivity for measurements on magnetic bearings with a large gap and a small displacement-range. By combining a differential scheme with two sensors, it is possible to measure both axial and radial displacements.

On the design of the sensor layout and the signal conditioning we achieve the following:

- High sensitivity of the sensor output relative to the measured displacement.
- Low sensitivity of the sensor output relative to the coupled variables, i.e. the current in the stator coils and sensor positioning.
- Decoupled measurements of the displacements in the axial and radial directions.

The principle scheme in fig. 3 shows two Hall-effect sensors which are placed on each lower pole of the electro-magnets where the measurement sensitivity to rotor movements is high and where stray effects are lower than on the upper poles. In fact the measurement of the flux density $\boldsymbol{B}$, at the lower pole, is not sensitive to the position of the sensor on the pole.

The output of the two Hall-effect sensors is sensitive to both axial and radial rotor displacements and is not sensitive to the rotation of the rotor.

Driving a hall-effect-sensor with a constant current i_h and placing the sensor in a magnetic field $\boldsymbol{B}$, the output voltage V_h generated by a Hall-effect sensor is proportional to the product of the flux density $\boldsymbol{B}$ and the current i_h.

In the magnets, the relation between ampere turns Θ and magnetic field strength H is given by the equation

$$\Theta = i\,n = \int_s \vec{H}\,ds = H_{fe} L_{fe} + H_g g_{(x,z)} \qquad (4.1)$$

where L_{fe} ist the length of the flux path in the iron and g is the length of the flux path in the airgap. The same relation expressed by the flux density $\boldsymbol{B}$ is

$$\Theta = i\,n = \frac{B}{\mu_o}\left(\frac{L_{fe}}{\mu_r} + g(x,z)\right) \qquad (4.2)$$

Since the relative permability of the iron is $\mu_r >> 1$, equation (4.2) can be simplified by the approximation

$$\Theta \approx i\,n = \frac{B}{\mu_o} g(x,z) \qquad (4.3)$$

Using (4.3) to express the flux density $\boldsymbol{B}$ for each side of the rotor leads to the equations

$$B_1 = n\,\mu_o\left(\frac{i_1}{g(+x,\pm z)}\right),\quad B_2 = n\,\mu_o\left(\frac{i_2}{g(-x,\pm z)}\right) \qquad (4.4)$$

Measuring B_1 and B_2 with the hall sensors we get the signals U_{h1} and U_{h2}. We replace B_1 and B_2 in (4.4) by the measured signals and we build the sum and the difference of these signals. Linearization of this relation in the working point $(i_x, i_y, x, z) = (0, i_{y0}, 0, 0)$ leads to the expressions for the displacement in radial and axial direction:

$$\hat{x} = C_x i_x + C_R\left(U_{h1} - U_{h2}\right) \qquad (4.5)$$

$$\hat{z} = C_y i_y + C_A\left(U_{h1} + U_{h2}\right) + C_0 \qquad (4.6)$$

where the coefficients C depends on the working point. The radial displacement signal mainly depends on the difference of the Hall-sensor signals and the axial displacement signal depends on the sum.

The design of an analog electronics circuit or a software signal processing to compute the equations (4.5) and (4.6) is relatively simple. Fig. 5 shows the block diagram of a

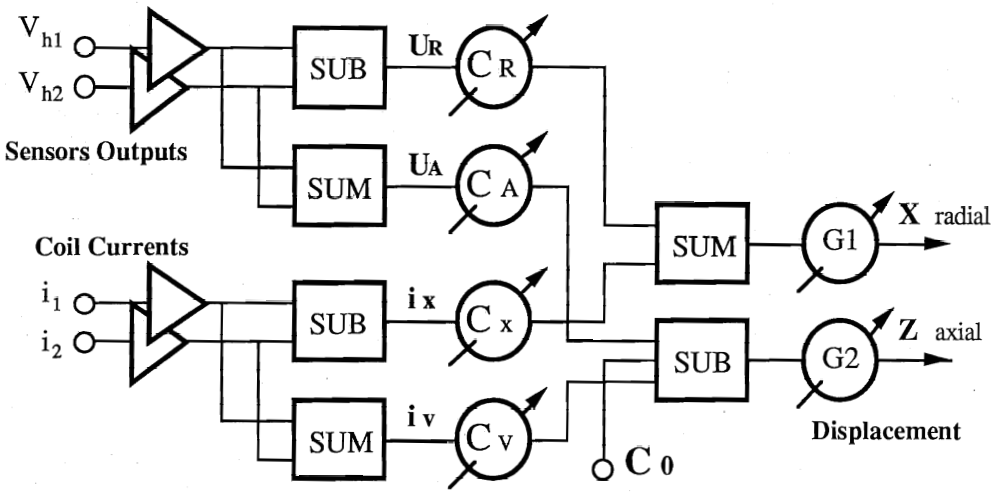

Fig. 5: *Sensors signal-conditioning*

realization which was built, using low cost operational amplifiers. The test results showed a high resolution and sufficient linearity. The cross-coupling between axial and radial displacements was approximately 5 %. A software realization even simplifies the tuning procedure of the coefficients.

5. Dynamic model and control concept.

Fig. 6 shows the functional blocks and the signal flow.of the closed-loop system, based on the flux density measurement. It can be seen that observing the rotor position is possible due to the mutual interaction of ***current***, ***flux*** and ***position*** in the plant.

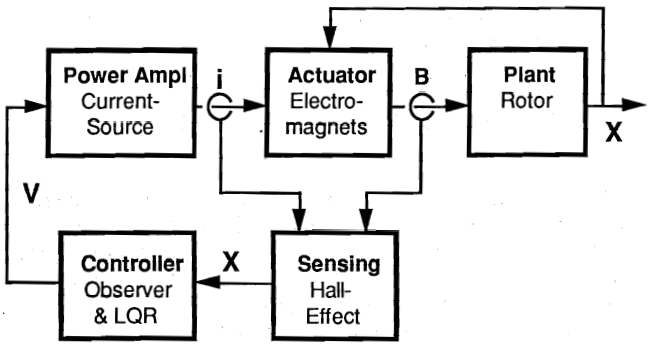

Fig. 6: *Principle control scheme*

For the dynamic model of the rotor, the coordinate system was defined as shown in fig. 7. The floating rotor as a free rigid-body has six degrees of freedom; three rotations (α,β,γ), and three translations (x,y,z). f_a and f_b are the forces of the two AMB's. The equations of motion have the well known form

$$M\ddot{\bar{s}} + P\dot{\bar{s}} + Q\bar{s} = N\bar{f} + V\bar{l} \qquad (5.1)$$

with $\bar{s} = (\alpha,x,\beta,y,\gamma,z)^T$

where M, P and Q are the coefficients of the autonomous rotor. **f** and **l** are vectors of the bearing and the load forces and moments.

Neglecting moments about the rotor axis Z_R, the forces acting on the rotor are the bearing controlled forces f_a and f_b and the rotor weight ***mg***. Each of the bearing forces can be separated into radial and axial components. The axial components are used to compensate the rotor weight and to control the axial position of the rotor. The radial components are used to control the radial position of the rotor.

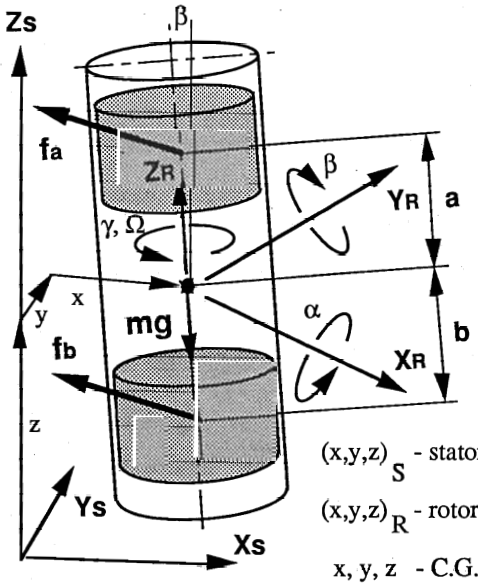

Fig. 7: *Rotor coordinates system*

The linear state-space model of the plant is developed, based on the model in [3]. Since radial and axial forces are decoupled, the model can be developed separately for the axial and radial directions.

In the radial direction for example, neglecting rotational harmonics, the dynamic model can be expressed with the state equations

$$\dot{\bar{x}} = \mathbf{A}\,\bar{x} + \mathbf{B}\,\bar{u} \tag{5.5}$$

$$\bar{y} = \mathbf{C}\,\bar{x} \tag{5.6}$$

With the state vector

$$\bar{x} = \left(x_a\ x_b\ y_a\ y_b\ \dot{x}_a\ \dot{x}_b\ \dot{y}_a\ \dot{y}_b\right)^T \tag{5.7}$$

and the control vector

$$\bar{u} = \left(i_{xa}\ i_{xb}\ i_{ya}\ i_{yb}\right)^T \tag{5.8}$$

With the dynamic model, the feedback controller can be designed to achieve the required performance, defined by the specifications. Since the observed variables are the rotor position, any of the existing and classical approaches can be adapted. One of these is based on the linear quadratic optimal regulator LQR, supplied with the full state, partly generated by a reduced order observer for the rotor position derivatives. Existing software packages can easily generate the observer and controller parameters based on the given model, and perform time simulation.

6. Computer Hardware and Software

A single board computer, based on a general purpose processor like Motorola MC680xx or based on a digital signal processor (DSP), is used. The processor is supported by input/output peripherals like D/A converters, A/D converters, parallel-port, communication device and timer. The structure of the computer system is shown in fig. 8.

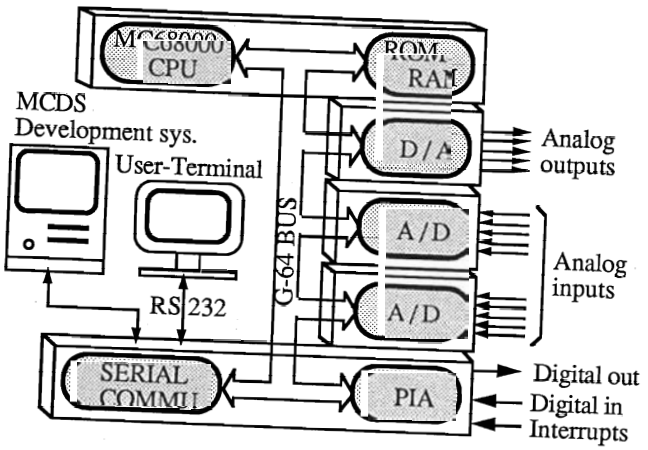

Fig. 8: *Structure of the omputer system*

The software is written in an high level language (Modula-2, C-language, etc.) on a personal computer using an appropriate development system. It is recommended to program the control equation in assembler to get a time optimale code and therefore a fast sampling rate. The object code is compiled and then down-loaded into the target system for execution.

The software is related to the hierarchy shown in fig. 9. Necessary procedures are imported to higher levels, from the low levels. The module '**Address**' holds the control-words locations of the complete hardware like: Timer, Serial-ports, A/D and D/A. modules.

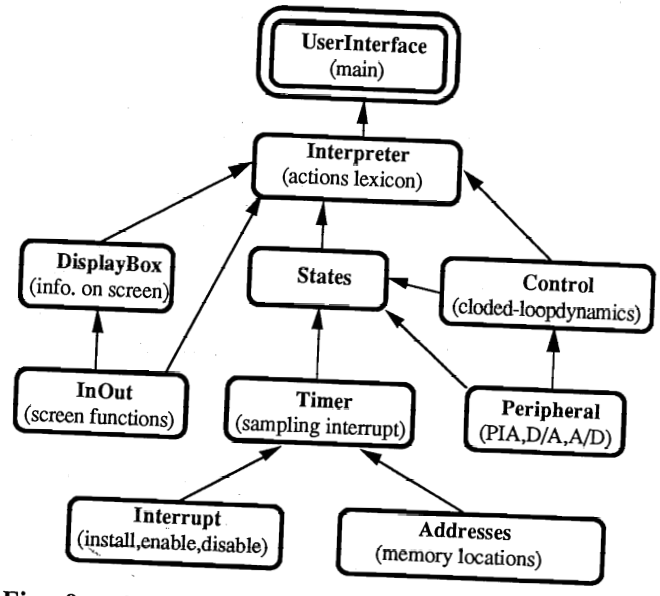

Fig. 9: *Software modules*

The modules '**Interrupt**', '**Timer**' and '**Peripheral**' are used to interact with the hardware, using a simple command format. The module '**Interrupt**' includes procedures to install, enable and disable interrupts. The module '**Timer**' includes procedures to start the timer with an externally defined time base and to stopp the timer. The timer interrupts the control process and defines the sampling rate.

The module '**Peripheral**' includes procedures which allow the use of analog and digital input/output ports with simple, single commands. E.g. this includes the control of each bit in the two eight bit parallel ports and each channel in the two A/D converters and in the D/A converter.

The module '**Control**' includes procedures to sample the rotor position signals, to transmit the current contol signals and to compute the closed-loop control algorithm, using imported procedures from the hardware level.

The module '**States**' contains procedures which select the requested system states mentioned in chapter 2.

The module '**Interpreter**' translates the user commands and executes them using procedures to read data from the terminal and display data on the screen. Tis procedures are imported from '**InOut**' and '**DisplayBox**'. The module '**UserInterface**' interacts with the user through a normal text terminal.

6. Implementation example: An AMB for a crystal-growth process.

The AMB system with the Hall-effect sensors ist suitable to support the rotor of a crystal-growth system. Fig. 10 shows a layout of the crystal-growth system. The crystal, fixed at the lower end of the rotor has to be pulled out of the melted metal or silicone. While pulling the crystal, the rotor has to be turned slowly to ensure a regular growth of the crystal.

The AMB suspension is carried vertically by an electro-mechanical actuator. The rotor is isolated inside a quartz tube, positioned and controlled in both axial and radial directions under special environmental conditions such as highly corrosive atmosphere and high temperature. For this kind of application which needs a very big airgap between rotor and magnets, the AMB with the hall-effect sensors are suitable

The important properties of this magnetic-bearing are a sufficient stiffness with a relatively large gap between rotor and stator, no separate axial bearing and a relatively low-cost realization.

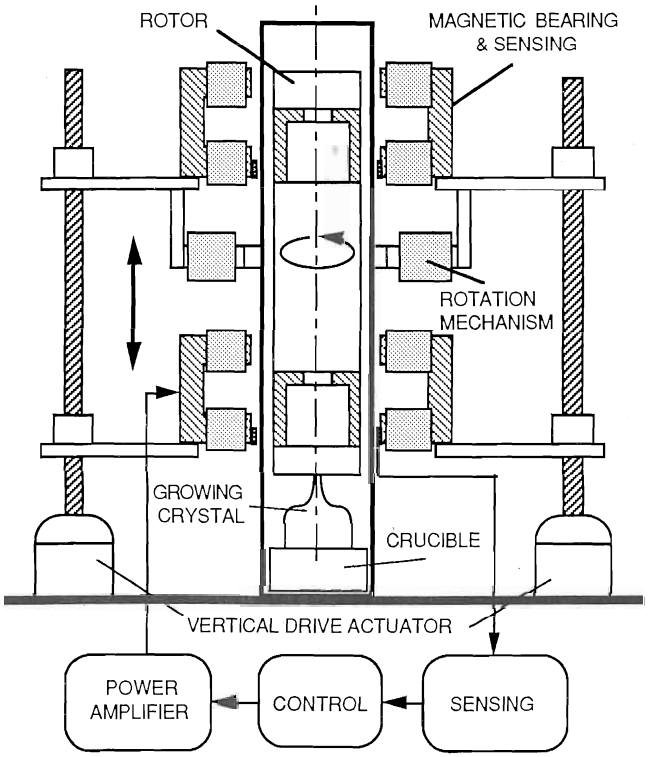

Fig. 10: *Construction layout of a crystal-growth system.*

The laboratory set-up which was designed, built and tested at the Institute for Robotics at ETH Zurich is shown in fig. 11. The system was realized, based on the preceding chapters. It performs satisfactory. Since in this application the rotation speed is very low, the velocity dependent coefficients of the plant model (in (5.5)) are neglected and the controller is decentralized, i.e. similar for all four radial directions.

The important characteristics are:

Mechanical:	Rotor dimensions:	Ø 80 x 600 L mm.
		Rotor weight: 3.5 Kg.
		Radial Gap: 17 mm.
Electrical:	Modular Switching Power Amplifiers 150 V x 15 A peak.	
Measurement:	Hall-sensors:	KSY 10 (Siemens)
	Signal conditioning:	Analog electronics.
Control:	Local LQR control with reduced order observer. Sampling frequency: 350 Hz.	
	Hardware:	MC 68000,Single-Board Computer
	Software:	Modula-2

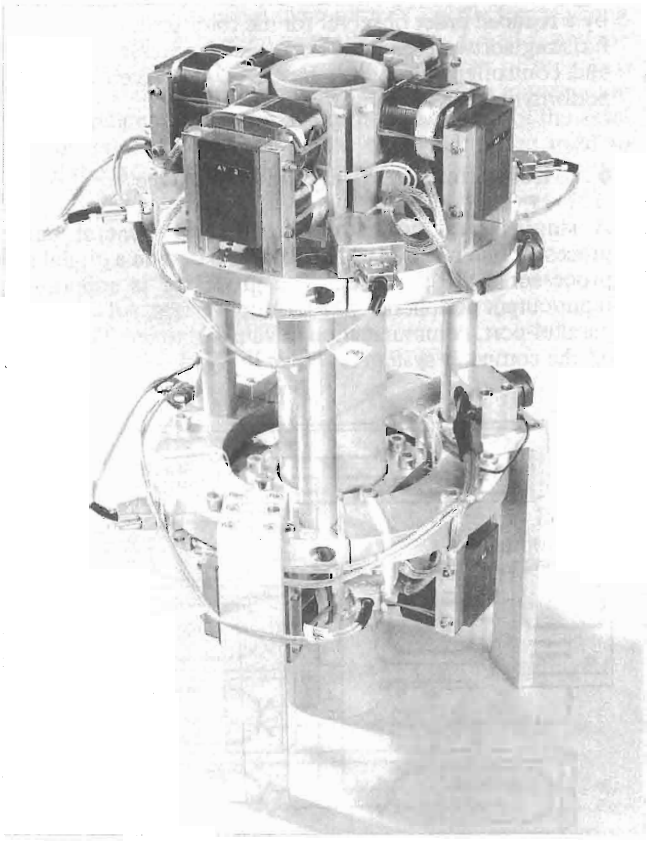

Fig. 11: *Laboratory set-up for AMB for the crystal-growth system.*

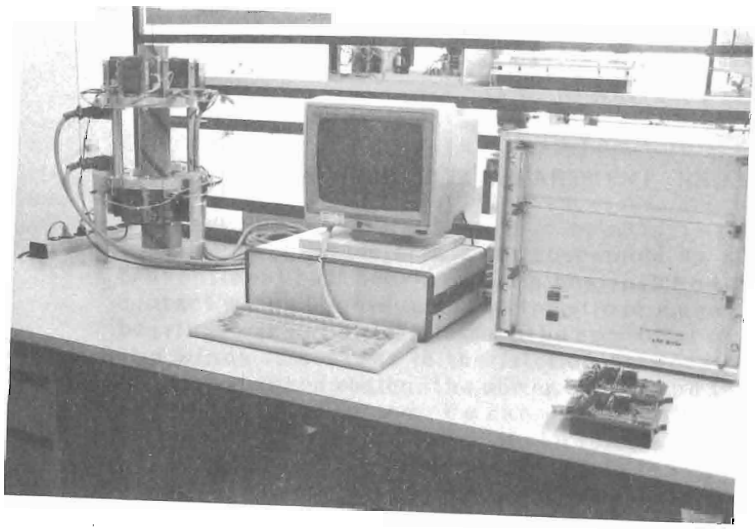

Fig. 12: *Laboratory set-up for AMB for the crystal-growth system.(Magnetic bearings,computer system and power amplifiers)*

7. Conclusions

A new way of using Hall-sensors to measure the rotor displacement in Active Magnetic Bearings was developed and tested. This measurement system shows good performance especially with a wide airgap It is simple and can be implemented at extremely low-costs.

A special setup of rotor and stator allows positioning and control of the rotor in both axial and radial directions *without* a a separate axial bearing.

A modular architecture of the computer system together with modular software and modular power amplifiers enables a straight forward and short time integration.

A laboratory setup of AMB for a crystal growth process was built and tested with satisfactory performance.

References:

[1] Schweitzer, G., H. Bleuler, A. Traxler, D. Vischer, D. Zlatnik: New Concepts for Low-Cost Mechatronics; Magnetic Bearing Example. Second IFAC Symposium on Low-Cost Automation, Milano, November 1989.

[2] Boden, K.: Wide-Gap, Electro-Permanent Magnetic Bearing System with Radial Transmission of Radial and Axial Forces. Proc. of the first Int. Symposium on Magnetic Bearings ETH Zurich, June 1988, Springer Verlag., 1989.

[3] Bleuler, H.: Decentralized control of a Magnetic Rotor Bearing System. Diss. ETH Nr. 7573, Zürich 1984.

[4] Traxler A.: Eigenschaften und Auslegung von berührungsfreien elektromagnetischen Lagern. Diss. ETH Nr. 7851, Zürich, 1985.

[5] Vischer, D.: Sensorlose und spannungsgesteuerte Magnetlager, Diss. ETH Nr. 8665, Zürich, 1988.